Electronic Supplementary Material (ESI) for Analytical Methods.
This journal is © The Royal Society of Chemistry 2024

Electronic Supplementary Information (ESI)

Characterizing a visual lateral flow device for rapid SARS-CoV-2 virus protein detection: pre-clinical and system assessment

Natpapas Wiriyachaiporn*[a], Jetnapang Kongrueng[a], Kannika Sukkuea[a], Rattana Tanrattanawong[a], Jarunee Vanichtanankul[b], Thanaya Saeyang[b], Tararat Jantra[b], Deanpen Japrung[a], Weerakanya Maneeprakorn[a], Suwussa Bamrungsap[a], Pareena Janchompoo[c] and Ekawat Pasomsub[c]

Experimental

Characterization of gold nanoparticle and the MAbs-GNP conjugate nanoprobes

To study the morphology and the size of the particles using TEM technique, the particles were diluted with distilled water in a 1:24 ratio and mixed for homogenization. Twenty microliters of the suspension were dropped into the carbon-coated 300 mesh copper TEM film grid and dried at 37 °C for 30 min. Subsequently, the grid of each sample was placed into the sample holder to begin measurement, and the TEM images were obtained by Transmission electron microscope (HT7800, HITACHI, Japan), with a voltage of 80 kV.

The hydrodynamic radius distribution and the zeta potential of the nanoparticles were measured using the DLS technique. The particle samples were diluted with distilled water, and a volume of 750 µl of sample suspensions in a microvolume quartz cuvette was performed triplicately for each sample at 25 °C using a DLS instrument (Zetasizer Nano ZS, Malvern, UK), with a wavelength of 633 nm of a helium-neon laser at an angle of 173.

UV-Vis spectroscopy was used to investigate the maximum absorption peak (A_{max}) value of the nanoparticles before and after conjugation. Briefly, a volume of 90 µl of each particle sample was transferred in triplicate, to a 96-well plate. UV-Vis absorption spectra of the nanoparticles were obtained at 25 °C in a wavelength range of 400-900 nm with 2 nm resolution using a microplate reader (Power wave XS2, Bio-Tek, USA).

Figure S1 A representative EDX spectra of elements obtained from **(a)** the test line (TL) of positive and **(b)** negative samples.

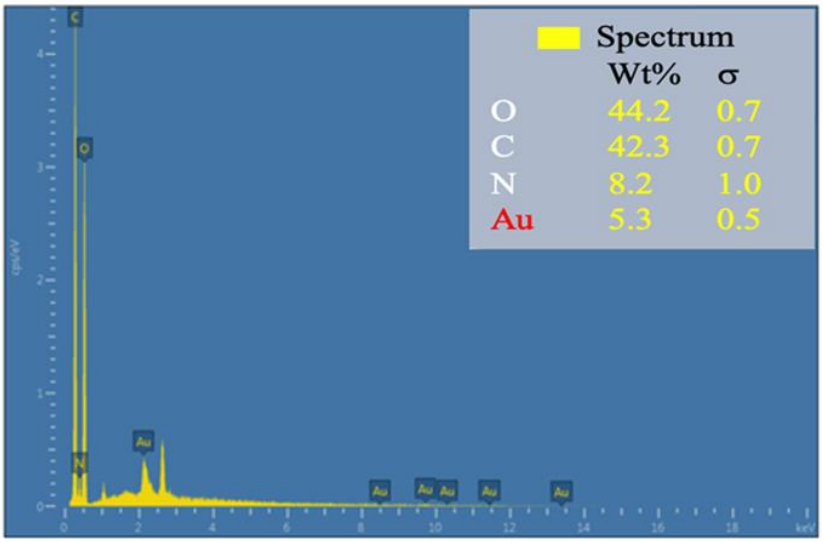

(A)

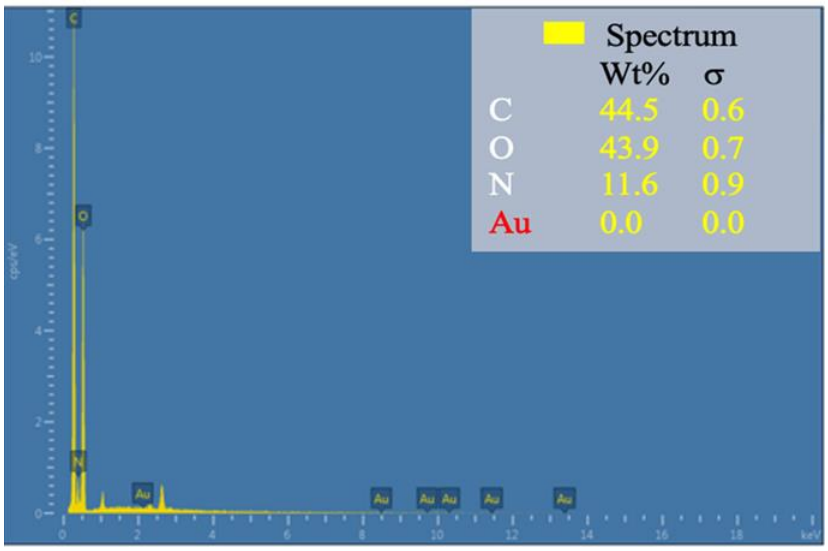

(B)

Figure S2 The change in size distribution, surface charge, and absorption spectra of the particles before and after conjugation, using TEM, DLS, UV-vis absorption spectra analyses. TEM images of gold nanoparticles **(a)** before, **(b)** after conjugation, and **(c)** in a presence of high salt concentration. *UV-vis* absorption spectra **(d)** of the particles at different conditions were demonstrated.

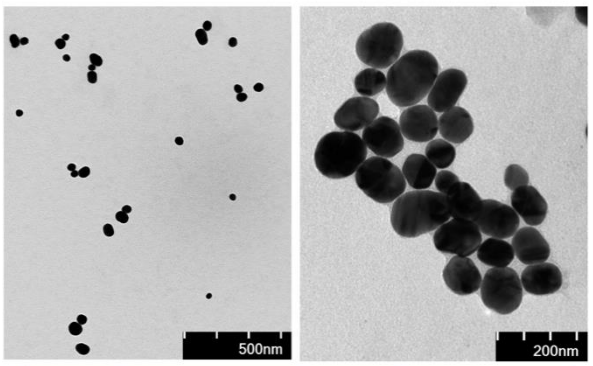

TEM	Size (nm)	DLS	Charge (mV)
	30.2 ± 4.7		-33.1 ± 2.5

(A)

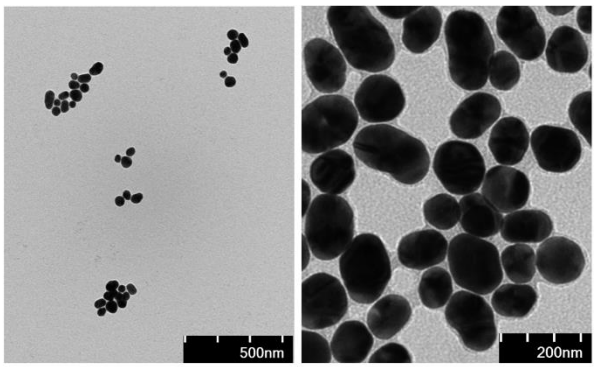

TEM	Size (nm)	DLS	Charge (mV)
	45.3 ± 4.7		-13.8 ± 1.5

(B)

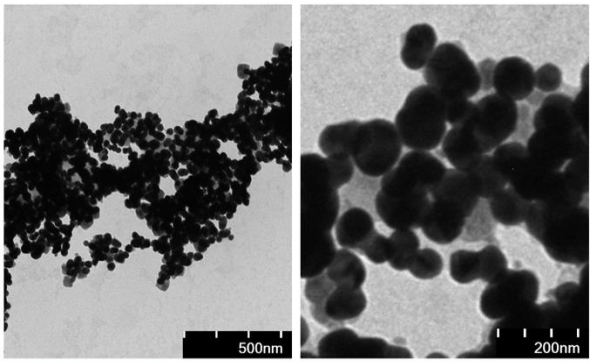

TEM	Size (nm)	DLS	Charge (mV)
	81.3 ± 8.6		-34.4 ± 0.9

(C)

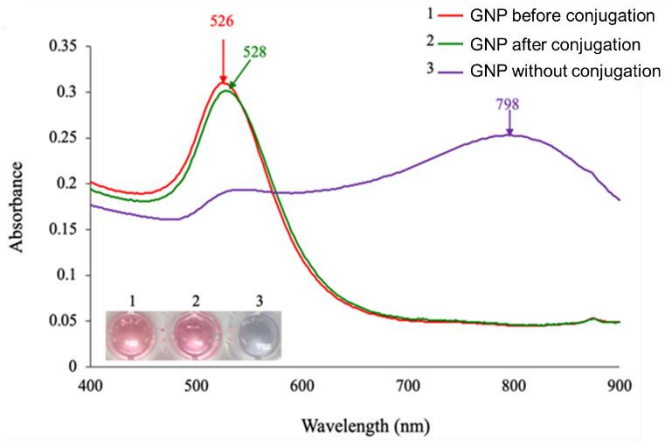

(D)

Figure S3 Coomassie staining of (a) 10 % SDS-PAGE of SARS-CoV-2 nucleocapsid protein and other closely related and non-related viral recombinant proteins and (b) Western blot analysis with primary antibody specific to SARS-CoV-2 nucleocapsid protein. Lane M: Ladder; Lane 1: Storage buffer (negative control); Lane 2: Recombinant SARS-CoV-2 nucleocapsid protein; Lane 3: SARS-CoV-2 spike protein; Lane 4: SARS-CoV nucleocapsid protein; Lane 5: MERS-CoV nucleocapsid protein; Lane 6: CoV-229E nucleocapsid protein; Lane 7: CoV-NL63 nucleocapsid protein; Lane 8: Recombinant influenza A nucleoprotein; Lane 9 Inactivated influenza B infected cell lysate protein; Lane 10: Inactivated respiratory syncytial virus infected cell lysate protein; Lane 11: Inactivated adenovirus infected cell lysate protein; Lane 12: Inactivated parainfluenza infected cell lysate protein

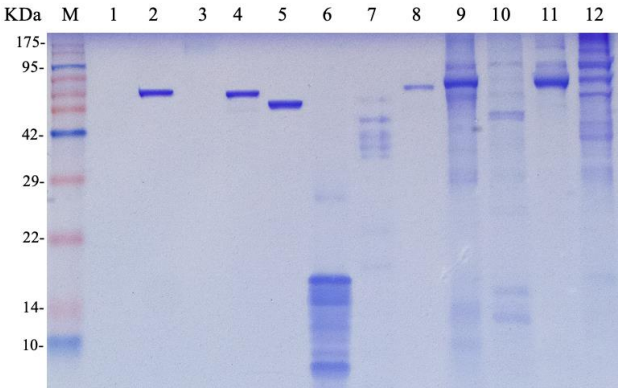

(A)

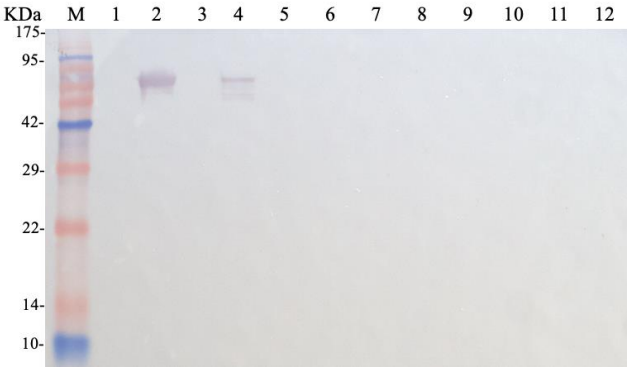

(B)

Figure S4 Performance correlation of the system in detecting SARS-CoV-2 nucleocapsids with other three commercially available rapid tests, including Test A and Test B (rapid test with direct signal visualization), and Test C (fluorescence based rapid test). Both semi-quantitative analysis (upper panel) and direct visualization (lower panel) revealed the performance of the developed system with the least limit of detection at 0.07 ng/test, compared to those of commercial Test A, B, and C (fluorescence-based test). With Test C, the result was obtained only in positive and negative format result, according to the instruction manual.

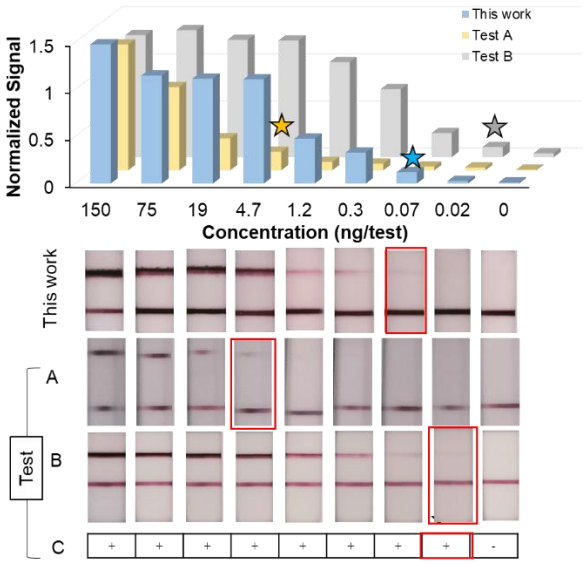

Table S1 Calculation of diagnostic parameters, including estimated sensitivity and specificity, predictive value of positive (PPV) and negative (NPV) results, and accuracy.

This work	**Reference method (Real-time RT-PCR)**		Total
	Condition Present	Condition Absent	
Positive	True Positive (TP)	False Positive (FP)	TP + FP
Negative	False Negative (FN)	True Negative (TN)	FN + TN
Total	TP + FN	FP + TN	All samples
Parameter Calculation			
Estimated sensitivity		100% × TP /(TP + FN)	
Estimated specificity		100% × TN /(FP + TN)	
Predictive value of a positive result (PPV)		100% × TP /(TP + FP)	
Predictive value of a negative result (NPV)		100% × TN /(FN + TN)	
Accuracy		100% × (TP + TN) /(TP + FN + FP + TN)	

Table S2 Preclinical evaluation of the system. Estimated sensitivity and specificity, predictive value of positive (PPV) and negative (NPV) results, and accuracy were shown.

This work	Reference method (Real-time RT-PCR)		Total
	Condition Present	Condition Absent	
Positive	49	0	49
Negative	1	100	101
Total	50	100	150
Parameter Calculation			
Estimated sensitivity			100% × 49 /(49 + 1) = 98%
Estimated specificity			100% × 100 /(0 + 100) = 100%
Predictive value of a positive result (PPV)			100% × 49 /(49 + 0) = 100%
Predictive value of a negative result (NPV)			100% × 100 /(1 + 100) = 99.001%
Accuracy			100% × (49 + 100) /(49 + 1 + 0 + 100) = 99.330%

148 **Table S3** Summary of recent LFIA-based and other approach as platforms for a detection of
149 SARS-CoV-2 nucleocapsid protein (Please see references for Table S3 at the bottom of the
150 page)
151

Biosensor	Biomarker	LOD/Performance	Detection time	Advantages	References
LFIA platform – colorimetric detection					
This work	N protein	LOD 0.7 ng.mL^{-1} Sensitivity: 98%, Specificity: 100%	15 min	-Rapid screening (15 min) & simple procedure -Direct visualization -First Screening (POC test)	This work
Previous works		LOD 2 ng.mL^{-1}, 50 PFU/Test Sensitivity: 85-98.6%, Specificity: 86-100%			(1), (2)
LFIA platform with other detection strategies (fluorescent, SERS, etc.)					
Fluorescent	N protein	LOD 0.01 ng.mL^{-1}	15-30 min	-Automated and user-independent analyzer	(3)
SERS-based		LOD 500 pfu.mL^{-1}	N/A	-High sensitivity, selectivity, reproducibility, and stability of the SERS platform -Reduces false-negative rate	(4)
LFIA platform integrated with nucleic acid amplifications methods (RPA, LAMP, CRISPR-Cas, etc.)					
LFIA with RPA	N gene	LOD 0.25 copies.mL^{-1}, 10 copies/reaction	10-60 min	- 100% accuracy in detecting SARS-CoV-2 - Accurate detection with no cross reactivity	(5), (6)
LFIA with LAMP		LOD 500 copies.mL^{-1}, Sensitivity: 87.1% Specificity: 100%	30 min	-Enables sensitive and reproducible detection of SARS-CoV-2.	(7)
LFIA with CRISPR-Cas		LOD 10 copies/test	1 h	-Consistent with RT-qPCR for clinical samples. -Can be applied in quantitative analysis of the virus	(8)
Non-LFIA based platforms					
Molecular Approach					
RT-PCR	N gene	LOD 250-500 copies.mL^{-1}	1-4 h	-Gold standard for COVID-19 testing.	(9)
RT-MCDA		LOD 5-6.8 copies/reaction Specificity: 100%	1 h	-High sensitivity & specificity. -Can be coupled with a nanoparticle-based biosensor	(10), (11)
LAMP		LOD 1-10 copies/reaction	1 h	- Increased sensitivity and specificity compared to RT-PCR	(12)

CRISPR-Cas		LOD 10 copies/reaction	30-90 min	-Portable nucleic acid-testing platform for early diagnosis -High sensitivity, selectivity, and low-cost	(13)
Other platforms (i.e., electrochemical, optical-based, SERS-based methods)					
Electrochemical immunosensor	N protein	LOD 0.4-0.8 $pg.mL^{-1}$	>15 min	- Low-cost and fast diagnostic tool -Initial testing results correlated with RT-PCR results.	(14), (15)
Optical-based methods		- *Microcantilever-based optical sensor*: LOD 0.71 $ng.mL^{-1}$ - *Optical Fiber Based Sensor Method*: LOD 100 $copies.mL^{-1}$	5-15 min	-Rapid, precise & sensitive detection of SARS-CoV-2 protein - Provide quantitative and qualitative assessments.	(16), (17)
SERS-based biosensor		LOD 10^{-6} $g.mL^{-1}$	N/A	-Long-range SERS biosensor for Simultaneous detection of SARS-CoV-2 nucleocapsid proteins. -High sensitivity, selectivity, reproducibility, and stability in human saliva and serum samples.	(18)

References (Table S3)

(1) D.R.P. Nicollete, R. Benedetti, B.A. Valença, K.K. Kuniyoshi, T.C. Schuartz de Jesus, A. Gevaerd, E.B. Santiago, B.M. Machado de Almeida, S.R. Rogal Júnior and M.V.M. Figueredo, *Sci Rep*, 2023, https://doi.org/10.1038/s41598-023-31641-5.

(2) S. Pickering, R. Batra, B. Merrick, L.B. Snell, G. Nebbia, S. Douthwaite, F. Reid, A. Patel, M.T. Kia Ik, B. Patel, T. Charalampous, A.Medina, M.J. Lista, P.R. Cliff, E. Cunningham, J. Mullen, K.J. Doores, J.D. Edgeworth, M.H. Malim, S.J.D. Neil and R.P. Galão, *Lancet Microbe*, 2021, doi: 10.1016/S2666-5247(21)00143-9.

(3) W. Chen, H. Chen, Y. Liu, H. Wei, Y. Wang, Z. Rong and X. Liu, *Anal Biochem*, 2022, doi: 10.1016/j.ab.2022.

(4) M. Lu, Y.J oung, , C.S. Jeon, S. Kim, D. Yong, H. Jang, S. H. Pyun, T. Kang and J. Choo, *Nano Converg.*, 2022, https://doi.org/10.1186/s40580-022-00330-w.

(5) T.R. Shelite, A.C. Uscanga-Palomeque, A. Castellanos-Gonzalez, P.C. Melby and B.L. Travi, *J Virol Methods*, 2021, doi: 10.1016/j.jviromet.2021.114227.

(6) Y. Sun, P. Qin, J. He, W. Li, Y. Shi, J. Xu, Q. Wu, Q. Chen, W. Li, X. Wang, G. Liu and W. Chen, *Biosens Bioelectron*, 2022, doi: 10.1016/j.bios.2021.113771.

(7) J. Tang, J. Zhu, J. Wang, H. Qian, Z. Liu, R. Wang, Q. Cai, Y. Fang and W. Huang, *BMC Infect Dis*, 2024, doi: 10.1186/s12879-023-08924-3.

(8) G. Su, M. Zhu, D. Li, M. Xu, Y. Zhu, Y. Zhang, H. Zhu, F. Li and Y. Yu, *Sens Actuators B Chem*, 2022, doi: 10.1016/j.snb.2022.132537.

(9) E. Kudo, B. Israelow, C.B.F. Vogels, P. Lu, A.L. Wyllie, M. Tokuyama, A. Venkataraman, D.E. Brackney, I.M. Ott, M.E. Petrone, R. Earnest, S. Lapidus, M.C .Muenker, A.J .Moore, A. C. Massana, Yale IMPACT Research Team; S.B. Omer, C.S.D. Cruz, S.F. Farhadian, A.I. Ko, N.D. Grubaugh and A. Iwasaki, *PLoS Biol*, 2020, doi: 10.1371/journal.pbio.3000867.

(10) J. Huang, X. Yang, L. Ren, W. Jiang, Y. Huang, Y. Liu, C. Liu, X. Chen and S. Li, *J Med Virol*, 2023, doi: 10.1002/jmv.28444.

(11) S. Li, W. Jiang, J. Huang, Y. Liu, L. Ren, L. Zhuang, Q. Zheng, M. Wang, R. Yang, Y. Zeng and Y. Wang, *Eur Respir J*, 2020, doi: 10.1183/13993003.02060-2020.

(12) J. Kashir and A. Yaqinuddin, *Med Hypotheses*, 2020, doi: 10.1016/j.mehy.2020.

(13) D. Huang, Z. Shi, J. Qian, K. Bi, M. Fang and Z. Xu, *Biotechnol Bioeng*, 2021, doi: 10.1002/bit.27673.

(14) S. Eissa, H.A. Alhadrami, M. Al-Mozaini, A.M. Hassan and M. Zourob, *Microchim Acta*, 2021, https://doi.org/10.1007/s00604-021-04867-1.

(15) S. Eissa and M. Zourob, *Anal Chem*, 2021, doi: 10.1021/acs.analchem.0c04719.

(16) D.K. Agarwal, V. Nandwana, S.E. Henrich, V.P.V.N. Josyula, C.S. Thaxton, C. Qi, L.M. Simons, J.F. Hultquist, E.A. Ozer, G.S. Shekhawat and V.P. Dravid. , *Biosens Bioelectron*, 2022, doi: 10.1016/j.bios.2021.113647.

(17) M.U. Hadi and M. Khurshid, *Sensors (Basel)*, 2022, doi: 10.3390/s22030751.

(18) Y. Dong, X. Yuan, K. Zhuang, Y. Li and X. Luo, *Anal Chim Acta*, 2024, doi: 10.1016/j.aca.2023.342070.